Eur. Phys. J. B **29**, 71–77 (2002)
DOI: 10.1140/epjb/e2002-00263-1

THE EUROPEAN PHYSICAL JOURNAL B

Specific heats of the charge density wave compounds o-TaS_3 and $(TaSe_4)_2I$

D. Starešinić[1,a], A. Kiš[1], K. Biljaković[1], B. Emerling[2,b], J. W. Brill[2], J. Souletie[3], H. Berger[4], and F. Lévy[4]

[1] Institute of Physics, PO Box 304, 10001 Zagreb, Croatia
[2] Department of Physics and Astronomy, University of Kentucky, Lexington, KY 40506-0055 USA
[3] CRTBT-CNRS, 38042 Grenoble Cedex 9, BP 166, France
[4] Institut de Physique Appliquée, EPFL, 1015, Lausanne, Switzerland

Received 5 April 2002 / Received in final form 28 June 2002
Published online 17 September 2002 –

Abstract. Specific heats of the charge-density-wave compounds o-TaS_3 and $(TaSe_4)_2I$ have been measured over the wide temperature interval 10 K–300 K. Both systems exhibit strong non-Debye behavior. Very weak and broad anomalies are observed at the Peierls transition temperatures. For o-TaS_3, the change in the curvature of the specific heat occurs at temperature of 40 K where glass transition has been deduced from dielectric measurements, and an extended scaling analysis suggests that the glass transition is associated with a dynamical cross over in length scales. We briefly discuss the characteristics and physical origins of the anomalies at both the Peierls and glass transitions.

PACS. 71.45.Lr Charge-density-wave systems – 65.40.Ba Heat capacity – 64.70.Kb Solid solid transitions – 64.70.Pf Glass transitions

1 Introduction

Although $(TaSe_4)_2I$ and o-TaS_3 (*i.e.* the orthorhombic polytype of TaS_3) are among the most widely studied of quasi one-dimensional (Q1D) systems undergoing Peierls transitions into charge-density-wave (CDW) states [1], their specific heats (c_p), particularly near these transitions, have not been adequately investigated. For both materials, there are reports of very low temperature (*i.e.* dilution refrigerator range) specific heats [2,3] and for o-TaS_3 there are differential scanning calorimetry results near the Peierls transition at $T_P = 215$ K which could not resolve an anomaly [4]. There are no reported specific heat results for $(TaSe_4)_2I$ near its Peierls transition temperature, which varies among samples between ≈240 K and 260 K [1].

Both systems exhibit very wide pretransitional fluctuations, associated with the opening of a pseudo gap at much higher temperatures than T_P, the 3D transition temperature [1], as expected for Q1D systems. These fluctuations make evaluation of thermodynamic behavior difficult, as one cannot safely guess the appropriate "background" behavior on either side of T_P. They also lead to a large enhancement of the ratio between the low-temperature gap and T_P [5]. In the case of $(TaSe_4)_2I$, an alternative strong electron-phonon coupling description has been proposed in which T_P corresponds to an ordering of a bipolaron fluid [7,8] in an order-disorder rather than the usual displacive transition. Inelastic neutron spectra [9] and diffuse X-ray scattering [10] showed almost no evidence for a soft-mode instability at T_P, as would be expected in a weak coupling picture, and a phenomenological model based on an optical-like order parameter was proposed [9]. For o-TaS_3, there have been no new structural investigations in the last decade, and its complicated atomic structure [11] remains undetermined.

In addition to very well known electronic transport features [1], the elastic signature of the Peierls transition has been demonstrated in low frequency measurements of Young's modulus [12–15] and the shear modulus [16], as well as in ultrasonic and thermal expansion studies [17]. In the related Q1D CDW compound, "blue bronze" ($K_{0.3}MoO_3$), anomalies in thermal expansion and Young's modulus at $T_P = 180$ K were found to be similar in shape to a cusp in the specific heat, as expected for continuous phase transitions, while an anomaly in the magnetic susceptibility was fit to their integral, *i.e.* the entropy [18]. These anomalies were analyzed in terms of both 3D-XY [18] and Gaussian fluctuations [19] of the CDW order parameter. One motivation for the present study was to determine if the comparisons applied to blue bronze could also be applied to $(TaSe_4)_2I$ and o-TaS_3. All three materials have relatively large, negative cusps in their chain direction Young's moduli, with anomalies of the order $\Delta E/E \sim -1\%$ (see below), although the anomaly in o-TaS_3 is wider and more symmetric than for the other materials [11–16,18]. Very different thermal

[a] e-mail: damirs@ifs.hr
[b] *Present address:* Department of Physics and Astronomy, SUNY-Geneseo, Geneseo, NY 14454, USA

anomalies might then be the signature of different microscopic CDW mechanisms, as mentioned above.

In addition, new evidence for the existence of a low-temperature CDW glass phase, which is reached at a glass transition at $T_g \sim T_P/4$ [20,21] increased our motivation for performing a wide temperature-range investigation of c_p. Any thermodynamic information obtained in the glass transition range will improve our understanding of this unusual phase, as well as general CDW properties beyond the classical microscopic picture.

2 Experimental

We have used a standard quasi-adiabatic heat pulse technique to measure the heat capacity of $(TaSe_4)_2I$ and o-TaS_3 in the wide temperature range, 10 K–300 K. In such a measurement, the sample was thermally linked to a temperature bath, which was kept at a well defined, stable temperature. The temperature of the sample relative to the bath was used to measure the heat capacity through the temperature jump after a heat pulse is applied to the sample [2].

Two samples of each material have been measured, each with a different thermometer. Most of the data shown below was taken with measurements made with a chromel – Au (0.07% Fe) thermocouple connected to a nanovoltmeter. The thermocouple sensitivity varies between 15 μV/K and 20 μV/K in this temperature range and the voltmeter noise for a proper reading rate was about 20 nV, resulting in 1–2 mK precision, comparable to the long term temperature stability of the sample. The amplitude of the temperature jump during a measurement was typically $\sim$0.5 K, so the possible precision of the measurement is about 0.2–0.4%.

Our tests have shown that the thermal link between the sample and the bath does not depend on the vacuum if the pressure is less than 10^{-6} mbar. Therefore, the vacuum in the sample holder was kept $\sim 10^{-7}$ mbar, in order to have a well-defined thermal link of the sample without any additional contribution from gas residue.

The o-TaS_3 sample consisted of thick carpet of $\sim 10^5$ needles, each $\sim$2 mm long with a cross-section of $\sim 10^{-4}$ mm^2. This carpet was hand-pressed to improve thermal contact and then wrapped with a copper foil around the thermocouple. A 50 μm constant wire that serves as a sample heater was wrapped around the foil and glued with 2–3 mg of GE varnish. The mass of o-TaS_3 was 97 mg, that of the copper foil 35 mg, and of the heater about 5 mg. The thermocouple wires as well as the heater wires served as a thermal link to the bath. Contribution of the addenda to the heat capacity was between 20% at low temperature and 30% at higher temperature.

For the second o-TaS_3 sample, a Cernox thermometer was used to measure the absolute sample temperature. The addenda contribution was larger for this sample, but the results were, although less precise, similar to those shown below.

$(TaSe_4)_2I$ was measured on two different solid polycrystalline chunks. Most of the results presented below are for sample 1, with mass $m_1 = 120$ mg, measured with the thermocouple. Sample 2 ($m_2 = 294$ mg) was measured with a platinum-chip thermometer; results for the two samples near T_P are compared in Figure 3a.

Experimental runs have been taken while both cooling and warming. Temperature intervals for taking data ranged from 0.5 K (at low temperature and near T_P) and 2 K elsewhere. Finally, small pieces of each sample have been used in electrical resistance measurements to characterize the sharpness of the Peierls transition.

3 Results

The measured specific heats of o-TaS_3 and $(TaSe_4)_2I$ in the whole temperature range are plotted in Figure 1. At room temperature, they approach the Dulong-Petit values (12 R for TaS_3 and 33 R for $(TaSe_4)_2I$, with R being the universal gas constant), as expected. Our high temperature results for o-TaS_3 agree with the differential scanning calorimetry (DSC) measurements of reference [4], as shown in the figure. At low temperatures, our data overlap well with that from references [2,3].

For 10 $K < T <$ 40 K, the specific heats of both samples are far from what would be expected from Debye theory for a crystal, with $c_p \propto T^2$ rather than the expected T^3 dependence. As discussed in [2], this weaker temperature dependence may result from a nearly dispersionless low frequency acoustic phonon mode propagating in the plane perpendicular to the conducting chains but polarized parallel to the chains [9,10,22]. Below 10 K, the T^3 behavior is recovered, but with correspondingly low Debye temperatures ($\sim$50 K for $(TaSe_4)_2I$ [2], and $\sim$130 K for o-TaS_3 [3]).

3.1 Specific heat peaks at the Peierls transitions

The inset to Figure 1 shows the specific heat near the phase transitions in enlarged scales. Anomalies at the Peierls transitions are certainly not obvious in these linear plots. This absence is roughly consistent with the simplest mean field estimates of the magnitudes of the anomalies. The resolution of our measurements in this temperature range is $\delta c_p \approx 0.03\ R$ for o-TaS_3 and 0.09 R for $(TaSe_4)_2I$. Assuming Fermi level electronic densities of states of $n_F \sim 0.44$ and 1.2 states/eV-molecule [23], one expects specific heat jumps ($\Delta c_{MF}/R = 4.7 n_F k_B T_{MF}$) of $\Delta c_{MF} \approx 0.04\ R$ and 0.11 R for o-TaS_3 and $(TaSe_4)_2I$, respectively, if $T_{MF} \sim T_P$; *i.e.* $\Delta c_{MF} \sim \delta c_p$.

However, specific heat anomalies at Q1D Peierls transitions are usually larger than their mean field estimates [1,18] because fluctuations typically lower T_P [5,6,23]. Furthermore, strong coupling to phonons, *e.g.* as has been suggested for $(TaSe_4)_2I$ [7,9], may result in large phonon contributions to Δc_p [24]. Therefore, the lack of apparent anomalies at T_P was initially surprising.

Part of the difficulty in finding small anomalies in the specific heat data is that there is no experimental way to separate the background behaviour (such as by applying

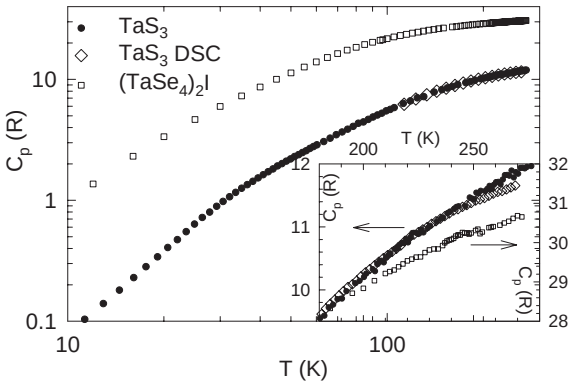

Fig. 1. Specific heat data of TaS_3 (full circles) of $(TaSe_4)_2I$ (empty squares) measured by the transient pulse technique in the temperature range 10 K–300 K. The previously published differential scanning calorimetry data of TaS_3 [4] (empty diamonds) are shown for comparison. In the inset are the same data presented in the restricted temperature range around the Peierls transition temperatures.

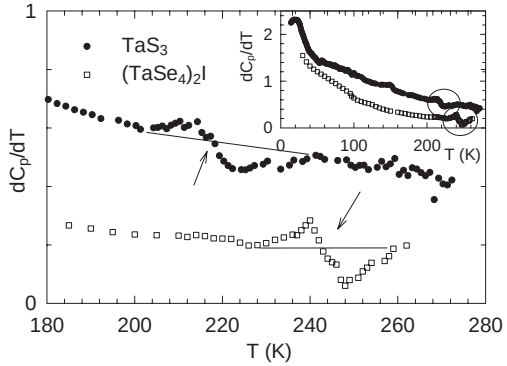

Fig. 2. The derivatives of the specific heats of TaS_3 and $(TaSe_4)_2I$ in the temperature range above 200 K reveal the existence of the cusp-like anomalies at the corresponding Peierls transition temperatures (arrows) and enable estimates of the widths of the transition regions (lines). The inset shows the derivatives in the entire temperature region covered by our measurements.

a magnetic field to a superconductor). In such a case, differentiation can be used to help isolate the anomalies. If there is indeed a small cusp in c_p at the Peierls transition, a zig-zag pattern should be present in $\mathrm{d}c_p/\mathrm{d}T$, which may be more readily observed. In Figure 2, we plot $\mathrm{d}c_p/\mathrm{d}T$ for both materials at temperatures near the transition, while the derivatives in the whole measured temperature range are shown in the inset. Indeed, zig-zag patterns are observed for both systems indicating that there are really cusp-like anomalies, near 220 K for o-TaS_3 and at 244 K for $(TaSe_4)_2I$. Although the features in the derivative can be seen at other temperatures as well, for instance at ∼150 K for o-TaS_3 and ∼90 K for $(TaSe_4)_2I$, they do not show the zig-zag pattern, which is therefore uniquely seen around Peierls transitons temperatures. The zig-zag patterns also allow us to estimate anomaly widths of about 20 K for both materials. In order to extract the critical parts of the specific heats at the Peierls transition temperatures we have estimated the normal baselines from the polynomial fits of the c_p data outside the regions around T_P defined by the anomaly widths. The critical parts are obtained as residues from the baselines subtraction in the anomalies width regions. It should be noted that different monotonic functions tried in order to estimate the baselines did not result in different values of the critical parts. The residues are presented in Figure 3a for $(TaSe_4)_2I$ (both samples) and in Figure 3b for o-TaS_3. The anomalies are $\Delta c_p \approx 0.1\ R$ and $0.04\ R$, respectively, comparable to the mean field estimates and the scatter in the data, as discussed above.

It should be pointed out that the above procedure only identifies local extrema in the specific heat. At CDW transitions, there is typically a (mean-field-like) change in baseline as well as a peak at T_P [18,25,26], and it is the baseline change that should be compared to model calculations [6,24]. Such a change in baseline may be mirrored in the elastic moduli [18,27], and has been clearly observed for Young's modulus of $(TaSe_4)_2I$ [13,15], but not for other

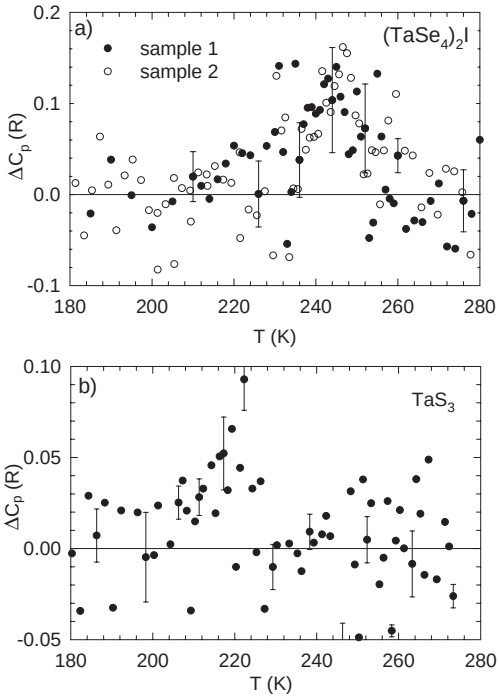

Fig. 3. The cusp-like excess contribution to the specific heat around the Peierls transition temperature of: a) $(TaSe_4)_2I$ (two samples), and b) TaS_3. Representative error bars are shown.

moduli of these materials [12,14,16,17]. Therefore, the magnitudes of the c_p anomalies shown in Figure 3 should only be considered rough estimates of the true anomalies.

In o-TaS_3, the small broad specific heat anomaly may be associated with broadening due to defects. A single crystal selected from the batch used for our c_p measurements had a resistive transition with a width of $\Delta T_{\mathrm{crit}} \approx$ 22 K, indicating these samples were slightly less pure than typical, nominally pure crystals, which have transition widths (obtained from resistivity [1]) of about 15 K. Resistivity measurements also indicated that T_P varied

from sample to sample between 212 K and 216 K for our crystals, which would also contribute slightly to the broadening of the transition in the heat capacity measurement.

Nonetheless, even taking into account the width of the anomaly, it is much smaller than would be expected on thermodynamic grounds. The anomaly in Young's modulus is comparable in width to that in the specific heat and has magnitude $\Delta E/E_0 \approx 1.2\%$ [14]. From the Ehrenfest relation [14,18,28],

$$\Delta c_{\text{Ehrenfest}} = -\left(\Delta E/E_0^2\right)\left(T_P M/\rho\right)\left(\frac{\mathrm{d}T_P}{\mathrm{d}\sigma}\right)^{-2} \qquad (1)$$

where ρ is the density, M the molecular weight, and σ uniaxial stress, one expects [14] $\Delta c_{\text{Ehrenfest}} = 0.18\ R$. Testardi [28] showed that the Ehrenfest relation will hold if the stress dependence of the anomalous free energy can be represented by

$$\Delta G = \varphi(\sigma)\, F\left(T - T_c(\sigma)\right) \qquad (2)$$

for differentiable functions φ and F. While equation (1) has been found to hold for CDW materials such as blue bronze [17] and quasi-two-dimensional $TaSe_2$ [26], it may fail for o-TaS_3, in which CDW properties have been found to be anomalously stress dependent [29], perhaps reflecting the possibility of "pulling the CDW into commensurability" with a small stress [29,30]. The fact that the anomaly in o-TaS_3 is inconsistent with Ehrenfest relation therefore suggests that equation (2) might not hold.

The situation is somewhat different in $(TaSe_4)_2I$, for which transport [1], elastic [13,15–17], and magnetic [23] anomalies in single crystals have been observed to be only ∼3 K wide. However, the variability among crystals, even from the same batch can be very wide; *e.g.* $T_P \sim (250 \pm 10)$ K. We therefore associate the width of our thermal anomaly primarily with a distribution of T_P's of the crystals constituting the samples. In this case, the magnitude of the anomaly for each crystal should be several time larger than the observed anomalies, *e.g.* Δc_p (single crystal) $\sim 0.7\ R \sim 6\Delta c_{MF}$. While such a large anomaly would seem to be consistent with a weak-coupled CDW transition suppressed by Q1D fluctuations, as discussed above, it is actually much larger than expected for this material. In McKenzie's model including Q1D fluctuations [6], the specific heat anomaly is given by

$$\Delta c_{\text{McKenzie}} = (1.9 \pm 0.7)(c/2\xi)R \qquad (3)$$

where ξ is the intrachain coherence length obtained from diffraction measurements at temperatures well above T_P [9], c is the longitudinal lattice constant, and the factor of 2 comes from the fact that there are two formula units per unit cell. The first numerical factor depends (inversely) on the strength of interchain coupling. Using $\xi \approx 10$ nm [9] and $c = 1.28$ nm [32] one finds $\Delta c_{\text{McKenzie}} \approx (0.1 \pm 0.04)\ R$; *i.e.* because of the long coherence length, the specific heat anomaly is not significantly enhanced above its mean-field value.

In fact, the coherence length is not very anisotropic [9], so it is not surprising that Q1D models fail. As mentioned above, it has been suggested that a strong coupling model involving bipolaron condensation might be more appropriate for $(TaSe_4)_2I$ [33]. In such a case, the specific heat anomaly should be enhanced by a lattice contribution. For example, MacMillan showed that phonon contributions increased the specific heat anomaly of two-dimensional 2H-$TaSe_2$ by a factor of 5 [24].

E_0 and $\mathrm{d}T_P/\mathrm{d}\sigma$ of $(TaSe_4)_2I$ have not been measured, so it is impossible to use equation (1) directly. However, from comparisons of measured anomalies in the thermal expansion coefficients (α) and ultrasonic moduli, Saint-Paul *et al.* [17] have estimated that the longitudinal stress dependence is unusually small: $\mathrm{d}T_P/\mathrm{d}\sigma \sim 0.06$ K/kbar. Using this value and their expansivity anomalies with the Ehrenfest relation

$$\Delta c_{\text{Ehrenfest}} = -\left(\Delta\alpha\right)\left(T_P M/\rho\right)\left(\frac{\mathrm{d}T_P}{\mathrm{d}\sigma}\right)^{-1} \qquad (4)$$

leads to an estimate of $\Delta c_{\text{Ehrenfest}} \sim 9\ R$! However, complicating their analysis are the facts that the modulus anomalies were sample dependent, and that different moduli have very different temperature dependences, making comparisons of their magnitudes difficult. Indeed, if the magnitude of the stress dependence is closer to that of the measured pressure dependence, $\mathrm{d}T_P/\mathrm{d}p \sim 1$ K/kbar [34], the Ehrenfest estimate would be close to our estimated value of Δc_p(single crystal). It has also been suggested [9] that the transition in $(TaSe_4)_2I$ may have first order character (in which case our measured specific heat anomaly would include contributions from latent heats distributed over a range of T_P's), in which case the Ehrenfest relations would not be expected to hold. Finally, very recent investigations confirmed the picture proposed in [9] the transition may be described as a Brillouin zone center Peierls instablity with mixed acoustic-optic character [35]. In addition to the acoustic-like modulation, the Ta tetramerisation with 10 times smaller amplitude has been found demonstrating uniqueness of the Peierls transition in $(TaSe_4)_2I$. The fact that it is not clear how to reconcile this picture with the polaronic interpretation of new ARPES measurements in the strong-coupling adiabatic limit [36] further demonstrates the very complex nature of the CDW transition and ground state in this system.

We continue with a discussion of the low temperature specific heat of TaS_3, and relate it to recent dielectric spectroscopy results.

3.2 Low temperature crossovers

As we have shown, the contribution associated with the critical behavior around the CDW transition ($\Delta c(T_P)$) is very small compared to the main lattice contribution and also within our experimental resolution. The critical contribution due to the glass transition observed in dielectric measurements at $T_g \sim T_p/4$ [20,21] is expected to be even smaller, as it takes place on the level of the superstructure; *e.g.* if the superstructure length scale is ξ and the

CDW coherence length is ζ, then $\Delta c(T_g) \sim \Delta c(T_p)$ $[\zeta_x\zeta_y\zeta_z / \xi_x\xi_y\xi_z] \sim 10^{-6}\Delta c(T_P)$, *i.e.* far beyond our resolution. On the other hand, as shown in the inset to Figure 2, there are distinct changes in the curvature of c_p near the expected glass transition temperatures. This led us to employ the data analysis based on the generalized scaling theory proposed by Souletie [37,38], which relies on a particular form of the derivative that both tests the applicability of the theory and enables the extraction of relevant parameters.

The generalized scaling analysis assumes that, with other thermodynamic variables, the specific heat exhibits "critical" behavior:

$$c_p T^2 \propto (1 - T_c/T)^{-\alpha} \tag{5}$$

but allows T_c to be negative for systems which, due to low dimensionality, strong correlations, or frustration [37], do not exhibit long-range order at finite temperatures. This temperature dependence of the specific heat reflects that of a correlation length which grows but stays finite with decreasing temperature [37].

From equation (5)

$$\frac{\mathrm{d}(\ln(T))}{\mathrm{d}(\ln(c_p T^2))} = \frac{T - T_c}{\alpha T_c}. \tag{6}$$

This linear temperature dependence can be used to test the applicability of the renormalization arguments, define its range of validity and finally give the value of the characteristic temperature T_c and the critical exponent α. We can also define another quantity called the initial interaction energy θ [37,38]:

$$\theta = (2 - \alpha)\, T_c \tag{7}$$

which represents the effective activation energy in the limit $T_c/T \to 0$ where $c_p \cdot T^2$ has an activated (Arrhenius) temperature dependence [38].

Different systems, such as glasses [38], ferromagnets, heavy fermions [37], and non-Fermi liquids [39] have been analyzed in this manner. Although this approach is rather unconventional and may seem speculative, the results of the analysis of o-TaS_3, like those for the materials mentioned above, are highly suggestive.

The results we have obtained by numerically differentiating our c_p data for o-TaS_3 according to equation (6) are presented in Figure 4. Below 200 K, a sequence of three regimes (labeled HT, MT and LT for high, medium and low temperature respectively) can be observed, each with a corresponding (negative) T_c and α. For the linear HT regime, 40 K $< T <$ 200 K, we find

$$T_c^{\mathrm{HT}} = -380 \text{ K}, \alpha^{\mathrm{HT}} = 4, \theta^{\mathrm{HT}} = 760 \text{ K},$$

while for the linear MT regime, 25 K $< T <$ 40 K, we find

$$T_c^{\mathrm{MT}} = -60 \text{ K}, \alpha^{\mathrm{MT}} = 6, \theta^{\mathrm{MT}} = 240 \text{ K}.$$

The LT regime below 25 K is actually best represented by the power law temperature dependence $c_p \propto T^{2.3}$.

The linearity in the MT and HT regions supports the scaling approach to the data analysis, and the crossover

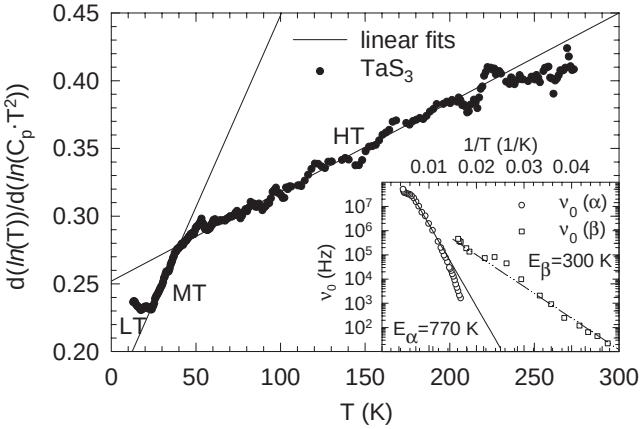

Fig. 4. Scaling derivative (see text) of the specific heat of TaS_3 in the entire temperature range. HT, MT and LT are the labels of the three distinct linear regions corresponding to the high, medium and low temperature region respectively. The lines are fits to the scaling expressions for the HT and MT regions of TaS_3. In the inset are the temperature evolutions of the relaxation frequencies (symbols) of two relaxation processes observed in the dielectric spectra [21] with the corresponding activation energies (solid lines).

between different regimes suggests a change in the scaling relations at the corresponding temperatures. As the crossover is not abrupt it can be regarded more as a kind of a glass transition than a thermodynamic phase transition [38]. Actually, this view can provide a strong link with the low frequency dielectric spectra [20,21] of the same system that we will discuss below.

The inset of Figure 4 shows the temperature dependence of the characteristic relaxation frequency ν_0 of two relaxation processes observed in the low frequency dielectric spectra of o-TaS_3 below T_P [20,21]. For the high temperature process, named the primary or α process, ν_0 starts to decrease slightly below T_p in an activated manner, with activation energy ≈770 K. However, at lower temperatures it tends to deviate towards stronger slowing down that leads to the finite freezing temperature $T_g \sim 40$ K, which is a sign of the glass transition at T_g. (T_g is defined as the temperature where the relaxation time exceeds the experimental time scales, conventionally taken as 10^3 s, so the corresponding frequency is 10^{-3} Hz). The second, or β process, becomes visible at temperatures slightly higher than T_g and follows an activated behavior far below T_g with the smaller activation energy ≈300 K. As we can see, there is a striking correspondence between the dielectric and c_p data: i) The crossover in c_p is situated at the temperature (40 K) where the freezing of the α process occurs. ii) The initial interaction energy θ^{HT} in HT region has the same value as the activation energy of the α process and θ^{MT} in the MT region has a value very close to the activation energy of the β process. iii) The β process apparently freezes at about 17 K (not shown in the inset, but see [20,21,40]), slightly below the crossover temperature between the MT and LT regions.

This correspondence would not be surprising if the dielectric response reflected dynamics of the lattice, since these dominate the thermal response. However, the dielectric response has been attributed solely to the CDW subsystem [20,21,40], which has been believed to affect only the phonons with wavevector near $2k_F$ that participate in the Kohn softening [41], which are a small fraction of the thermal phonons in the case of weak electron-phonon coupling [24], assumed to be the main mechanism of CDW formation. Our results therefore lead us to question this assumption. We have presented arguments [21] that the freezing of the α process is a result of a strong *intra-CDW* Coulomb interaction that takes place when the screening by free carriers becomes ineffective as they freeze out at low temperatures. It seems now that the stiffening of CDW and the freezing of CDW disorder also affect the phonon dynamics. In the view of the generalized scaling analysis this occurs through a change in the localisation, *i.e.* correlation length, of the phonons. The influence of the CDW on the host lattice has also been shown in recent structural studies in some other CDW systems. In blue bronze ($K_{0.3}MoO_3$), pronounced changes in the host lattice parameters have been observed [42] in the temperature region close to the glass transition detected in dielectric spectroscopy [43] and thermally stimulated discharge measurements [21,43–45]. In $(NbSe_4)_{10}I_3$, a continuous monoclinic deformation of the host lattice below T_P has been attributed to shear elastic strain coupling to the CDW [46], and similar observations have been made in $(TaSe_4)_2I$ [47]. Additionally the fact that elastic moduli of CDW systems change strongly when the CDW is depinned [15,48] also implies a strong CDW-phonon coupling. Finally, Golovnya *et al.* [49] have shown that thermal contraction of o-TaS_3 lattice is affected by deformation of the CDW.

The growing phonon correlation length, which enables the application of the generalized scaling approach, would be a consequence of the growing dynamic correlation length of the CDW. In the scaling hypothesis, the critical exponent α of c_p is related to the dimensionality d and the critical exponent ν of the correlation length growth as [37,38]:

$$\alpha = 2 - \mathrm{d}\nu. \tag{8}$$

For temperatures above $T_g \sim 40$ K, we have $\alpha^{\mathrm{HT}} \approx 4$, while for low temperatures below T_g we have have $\alpha^{\mathrm{MT}} \approx 6$. Therefore, we obtain the ratio:

$$\frac{(d\nu)^{\mathrm{HT}}}{(d\nu)^{\mathrm{MT}}} = \frac{2-\alpha^{\mathrm{HT}}}{2-\alpha^{\mathrm{MT}}} \cong 0.5. \tag{9}$$

If the critical exponent for the correlation length does not change, this would imply that the effective dimensionality changes form $d = 2$ below T_g to $d = 1$ above. This type of dimensional crossover is typical for weakly coupled layered (or chained) structures for which, as the temperature decreases the coherence volume increases sufficiently to make the interchain (or interlayer) coupling effective, thus increasing the dimensionality of the system. We suggest that the increasing Coulomb interaction effectively couples the phonon dynamics on different TaS_3 chains at low temperatures. The strong influence of the CDW can also be inferred from the LT power low exponent of 2.3. This non-Debye value implies either a lower dimensionality, as discussed above, or an additional contribution(s) in this temperature range. A strong CDW contribution is also present at much lower temperatures [2,3], where the phonon contribution is almost negligible, so there is no need to invoke the CDW-phonon coupling.

We have applied the same analysis to the c_p data of $(TaSe_4)_2I$. We did not observe strictly linear regimes. Nonetheless, there is a distinct feature near 90 K (as seen in the inset of Fig. 2), not far from the temperature at which a peak in the thermally stimulated discharge current has been observed [45], and such a peak is usually an indication of the freezing of the dielectric relaxation process. However, in order to resolve this, a detailed dielectric spectroscopy investigation of $(TaSe_4)_2I$ is needed, as the system exhibits complex features associated with a mixed ground state, as discussed at the end of previous subsection.

4 Conclusion

We have measured the specific heats of the charge-density-wave (CDW) materials $(TaSe_4)_2I$ and TaS_3 between 5 K and 300 K using pulsed calorimetry. These are the first measurements of the specific heats of the two materials in such a wide temperature range, particularly for $TaSe_4)_2I$, for which data only below 7 K had been published. Also, the existence of the cusp-like anomalies at the Peierls transition temperatures has been shown for the first time. The size of the anomaly for o-TaS_3 is smaller than expected on the basis of other thermodynamic measurements, but that for $(TaSe_4)_2I$ is of the magnitude expected for a less-anisotropic, strongly coupled system. The generalized scaling analysis reveals the presence of a crossover anomaly at 40 K in TaS_3, which can be related to the glass transition observed at a similar temperature in dielectric spectroscopy measurements. The fact that the glass transition on the level of the CDW superstructure affects the specific heat, governed essentially by phonons in this temperature range, leads to the surprising conclusion that the interaction between CDW and the phonons is not negligible below T_P. We have discussed briefly the microscopic origin of these features within the context of CDW models.

We wish to thank P. Monceau for his continuous support and for providing us with the large samples of $(TaSe_4)_2I$. This research was funded in part by the NSF, through an international program supplement to award #DMR-9731257. One of us (B.E.) acknowledges the hospitality of the Institute of Physics during her 4 months stay in the final part of this study.

References

1. P. Monceau, in *Electronic Properties of Inorganic Quasi-One-Dimensional Compounds, Part II: Experimental*, edited by P. Monceau (Kluwer Academic, Dordrecht, 1985), p. 137; G. Gruner, Rev. Mod. Phys. **60**, 1129 (1988); G. Gruner, *Density Waves in Solids* (Addison-Wesley, New York, 1994)
2. K. Biljaković, J.C. Lasjaunias, F. Zougmore, P. Monceau, F. Levy, L. Bernard, R. Currat, Phys. Rev. Lett. **57**, 1907 (1986)
3. K. Biljaković, J.C. Lasjaunias, P. Monceau, F. Levy, Europhys. Lett. **8**, 771 (1989)
4. Y. Wang, M. Chung, T.N. O'Neal, J.W. Brill, Synth. Met. **46**, 307 (1992)
5. P.A. Lee, T.M. Rice, P.W. Anderson, Phys. Rev. Lett. **31**, 462 (1973)
6. R.H. McKenzie, Phys. Rev. B **51**, 6249 (1995)
7. S. Aubry, P. Quemerais, in *Low-Dimensional Properties of Molybdenum Bronzes and Oxides*, edited by C. Schlenker (Kluwer Academic, Dordrecht, 1989), p. 295
8. S. Aubry, G. Abramovici, J.L. Raimbault, J. Stat. Phys. **67**, 675 (1992)
9. J.E. Lorenzo, R. Currat, P. Monceau, B. Hennion, H. Berger, F. Levy, J. Phys. Cond. Matt. **10**, 5039 (1998)
10. S. Ravy, R. Moret, Synth. Met. **120**, 1065 (2001)
11. C. Roucau, R. Ayroles, P. Monceau, L. Guemas, A. Meerschaut, J. Rouxel, Phys. Stat. Sol. (a) **62**, 483 (1980)
12. J. W. Brill, Solid State Commun. **41**, 925 (1982)
13. A. Suzuki, M. Mizubayashi, S. Okuda, J. Phys. Soc. Jpn **57**, 4322 (1988)
14. G. Mozurkewich, R. Jacobsen, Synth. Met. **60**, 137 (1993)
15. G. Mozurkewich, in *Perspectives in Physical Acoustics*, edited by Y. Fu *et al.* (World Scientific, Singapore, 1992), p. 237
16. H.R. Salva, A.A. Ghilarducci, P. Monceau, F. Levy, D'Anna, W. Benoit, Solid State Commun. **94**, 41 (1995); H.R. Salva, A.A. Ghilarducci, F. Levy, Solid State Commun. **100**, 673 (1996)
17. M. Saint-Paul, S. Holtmeier, R. Britel, P. Monceau, R. Currat, F. Levy, J. Phys. Cond. Matt. **8**, 2021 (1996)
18. J.W. Brill, M. Chung, Y.-K. Kuo, X. Zhan, E. Figueroa, G. Mozurkewich, Phys. Rev. Lett. **74**, 1182 (1995)
19. M. Chung, Y.-K. Kuo, X. Zhan, E. Figueroa, J.W. Brill, G. Mozurkewich, Synth. Met. **71**, 1891 (1995)
20. D. Starešinić, K. Biljaković, W. Brütting, K. Hosseini, P. Monceau, H. Berger, F. Levy, Phys. Rev. B **65**, 165109 (2002)
21. D. Starešinić, Ph.D. thesis, University of Zagreb, Zagreb and University J. Fourier, Grenoble 2000
22. H. Fujishita, S. M. Shapiro, M. Sato, S. Hoshino, J. Phys. C. **19**, 3049 (1986)
23. D.C. Johnston, M. Maki, G. Gruner, Solid State Commun. **53**, 5 (1985)
24. W.L. McMillan, Phys. Rev. B **16**, 643 (1977)
25. D.K. Powell, T. Miebach, S.-L. Cheng, L. K. Montgomery, J.W. Brill, Solid State Commun. **104**, 95 (1997)
26. M. Barmatz, L.R. Testardi, F.J. DiSalvo, J.M.E. Harper, Phys. Rev. B **13**, 4637 (1976)
27. M. Barmatz, L.R. Testardi, F.J. DiSalvo, Phys. Rev. B **12**, 4367 (1975)
28. L.R. Testardi, Phys. Rev. B **12**, 3849 (1975)
29. V.B. Preobrazhensky, A.N. Taldenkov, S.Yu. Shabanov, Solid State Commun. **54**, 399 (1985)
30. T.A. Davis, W. Schaffer, M.J. Skove, E.P. Stillwell, Phys. Rev. B **39**, 10094 (1989)
31. Z.G. Xu, J.W. Brill, Phys. Rev. B **43**, 11037 (1991)
32. P. Gressier, L. Guemas, A. Meerschaut, Acta Cryst. B **38**, 2877 (1982)
33. H. Requardt, R. Currat, P. Monceau, J.E. Lorenzo, A.J. Dianoux, J.C. Lasjaunias, J. Marcus, J. Phys. Cond. Matt. **9**, 8639 (1997)
34. L. Forro, H. Mutka, S. Bouffard, J. Morillo, A. Janossy, Lect. Notes Phys. **217**, 361 (1985)
35. V. Favre-Nicolin, S. Bos, J.E. Lorenzo, J.-L. Hodeau, J.-F. Berar, P. Monceau, R. Currat, F. Levy, H. Berger, Phys. Rev. Lett. **87**, 015502 (2001)
36. L. Perfetti, H. Berger, A. Reginelli, L. Degiorgi, H. Höchst, J. Voit, G. Margaritondo, M. Grioni, Phys. Rev. Lett. **87**, 216404 (2001)
37. J. Souletie, J. Phys. France **49**, 1211 (1988)
38. J. Souletie, J. Phys. France **51**, 883 (1990)
39. J. Souletie, Y. Tabata, T. Taniguchi, Y. Miyako, Eur. Phys. J. B **8**, 43 (1999)
40. F. Ya. Nad', P. Monceau, Solid State Commun. **87**, 13 (1993); F. Nad', P. Monceau, Phys. Rev. B **51**, 2052 (1995)
41. W. Kohn, Phys. Rev. Lett. **2**, 393 (1959)
42. M. Tian, L. Chen, Y. Zhang, Phys. Rev. B **62**, 1504 (2000)
43. K. Hosseini, W. Brütting, M. Schwörer, E. Riedel, S. Van Smaalen, K. Biljaković, D. Starešinić, J. Phys. IV France **9**, Pr10-41 (1999)
44. R.J. Cava, R.M. Fleming, E.A. Rietman, R.G. Dunn, L.F. Schneemeyer, Phys. Rev. Lett. **53**, 1677 (1984)
45. D. Starešinić, K. Biljaković, N.I. Baklanov, S.N. Zaitsev-Zotov, Synth. Metals **103**, 2130 (1999)
46. Z. Vučić, J. Gladić, C. Haas, J.L. DeBoer, J. Phys. I France **6**, 265 (1996)
47. Z. Vučić (private communication)
48. X. Zhan, J.W. Brill, Phys. Rev. B **56**, 1204 (1997)
49. A.V. Golovnya, V.Ya. Pokrovskii, P.M. Shadrin, Phys. Rev. Lett. **88**, 246401 (2002)